CHAPTER 6

Efficient Mass Correction Using an Adaptive Method

Wolfgang Szwillus and Hans-Jürgen Götze
Christian Albrechts University, Kiel, Germany

6.1 INTRODUCTION

The gravity effect of topography veils the gravity signal coming from deeper sources. The process of removing the gravity effect of topography is called "mass correction." Although the necessity to correct for the influence of topography on gravity has been recognized already in the 19th century, progress in this area continues. For instance, Mikuška et al. (2006) have challenged the convention, that only topography up to a distance of 167 km from the station is relevant (see e.g., Bullard, 1936; LaFehr, 1991). They proposed to calculate the "distant relief effect" (DRE), which refers to the gravity of topography beyond a correction radius of 167 km, and found long wavelength, yet significant contribution of distant relief.

The DRE is less important for density modeling at a local exploration scale because long wavelength trends are removed during regional–residual separation (e.g., Nabighian et al., 2005). However, for modeling deep and/or extensive structures, accurate removal of long wavelength effects is critical. These wavelengths are now provided with unprecedented accuracy by satellite measurements (Bouman et al., 2015).

Therefore, a new algorithm for topographic correction should be able to calculate the mass correction from global topography or at least from large areas. Furthermore, it must correct ground, airborne, and satellite measurements consistently. Thus, it must also be capable of handling high-resolution topographic data efficiently.

Mass correction can be calculated directly, or in two steps (giving the same result). In the two-step procedure, first a "Bouguer correction" is applied, which assumes topography is an infinite flat slab, with

Understanding the Bouguer Anomaly. DOI: http://dx.doi.org/10.1016/B978-0-12-812913-5.00005-1

thickness equal to the station height. Afterward, a "topographical correction" is carried out, which corrects for the difference between real topography and the assumed slab. The adaptive method (Szwillus, 2014) we propose works with either convention, but we prefer the one-step procedure because it is conceptually simpler.

All methods for topographic correction based on digital elevation models (DEMs) work essentially the same way: Each grid cell of the DEM is translated into an elementary volume, for example, into a flat-top prism. Repeating this for all grid cells gives a volumetric model of topography. One of the earliest papers which describe the application of DEMs for gravity-field corrections was the one of Cogbill (1990). To calculate the gravity effect of such a volume model, topographic and bathymetric densities are needed. Typically, constant densities of 2670 and 1630 kg/m^3, respectively, are assumed. Existing methods make use of different elementary volumes e.g., cylinder segments (Hayford and Bowie, 1912; Hammer, 1939), prisms (Nagy et al., 2000), or tesseroids (Grombein et al., 2013). Generally, there exist several ways to calculate the gravity effect of a volume: closed analytical solutions, analytical estimation by Taylor series, or numerical integration (Heck and Seitz, 2007).

For any method, the number of calculations is proportional to the number of pairs of grid-points and stations. Accordingly, if the topographical grid contains $X \times Y$ cells, and there are N stations, a total of $X \times Y \times N$ pairs need to be calculated. Increasing the resolution or horizontal grid extent, and therefore, the number of nodes in the grid makes the calculations a lot more time consuming.

To reduce the processing time, we propose an adaptive approach that uses the gravity field itself as a way to determine the necessary resolution. Starting with a coarse grid for representation of topography, the resolution is increased locally, until a further increase of resolution would only change the obtained topographic effect negligibly.

The aim of this work is to demonstrate the advantage of the adaptive approach over earlier applications. It needs only a fraction of the computational time and still results in sufficiently accurate value for gravity-field corrections.

6.2 PRINCIPLE OF ADAPTIVE ALGORITHM

Hayford and Bowie (1912) already used a variable resolution representation of topography over hundred years ago. The cylinder compartments are getting larger as one moves away from the gravity station due to the $1/r^2$ numerical effect of the gravity field decay. We build on this approach, but change the size of the elementary bodies (i.e., the resolution) automatically, instead of defining an a priori size. In essence, the calculation of the gravity effect of many small elementary bodies is replaced by calculating fewer but partly larger blocks.

6.2.1 Variable resolution representation of topography

Quadtrees (Samet, 1990) provide an elegant way to create variable resolution representations of a grid. Here, a topographic grid, called the base grid, is used as input. For simplicity's sake, we will assume the base grid is square and contains $2n$ values in each dimension. Then the associated quadtree consists of $n + 1$ layers. Each layer contains nodes that correspond to rectangular cells (Fig. 6.1 and 6.2). Every node stores the topographical height and density of its corresponding cell.

The nodes of the different layers are in a hierarchical relation. This is achieved by constructing the quadtree from bottom up. The cells of layer $j + 1$ are created by merging four neighboring cells of layer j. Conversely, the cells of layer j can be obtained by splitting the cells of layer $j + 1$. Let N be a node of layer $j + 1$, then four nodes from layer j exist, that were used to construct node N (see Fig. 6.1). These four nodes C1, C2, C3, and C4 are the children of N. Similarly, N is called the parent of C1 to C4. The top layer (layer n) contains only one node, called the root (note that the root is at the top of the tree!). Its density

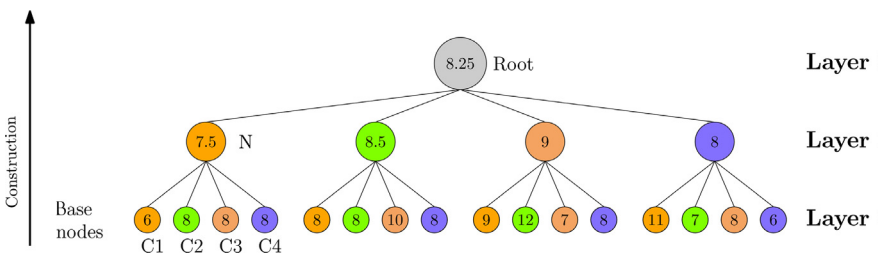

Figure 6.1 Tree representation of the topography. Colors are used to mark corresponding grid cells in Fig. 6.2. The values of the nodes in layer 1 are obtained by averaging over four nodes of layer 0 (cells of the base grid). Likewise is the final calculation for the single node in layer 2, which is the root of this tree. Thus, the tree is constructed from bottom up. Note that the root is at the top of tree.

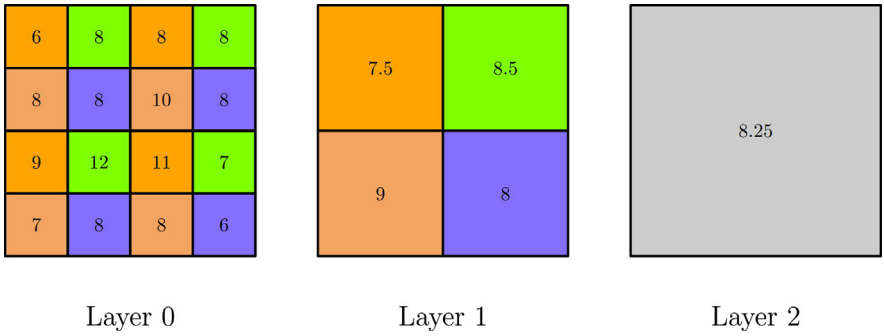

Figure 6.2 Grid representation of topography at different resolutions. The cells of layer 1 are obtained by averaging over four cells of layer 0, and likewise for layer 2 (gray in print versions).

and height are equal to the average density and height of the entire region.

Each layer has half the resolution of the layer below it. Thus, a quadtree essentially represents a set of n grids at different resolution steps. These grids are nested in such a way that the resolution can be changed locally without affecting other parts of the grid.

The heights and densities stored in the nodes of layer $j+1$ have to be computed by averaging four nodes of layer j. The topographical mass belonging to a single node is approximately:

$$m_i = A_i h_i \rho_i$$

where A_i is the area, h_i is the height, and ρ_i is the density of each children cell i ($i = 1.4$). Area, height, and density of the parent cell ($\overline{A}$, $\overline{h}$, and $\overline{\rho}$) must be determined from the children in such a way that total mass topographic mass is conserved. This guarantees an optimal approximation of the gravity effect by the higher layers.

The area of the parent cell is just the sum of the children's areas:

$$\overline{A} = \sum_i A_i$$

We ensure mass conservation by first calculating the density of the parent cell, using area-weighted averaging:

$$\overline{\rho} = \frac{\sum_i A_i \rho_i}{\sum_i A_i} = \frac{\sum_i A_i \rho_i}{\overline{A}}$$

Then, we calculate the height of the parent cell by averaging height weighted with area and density:

$$\overline{h} = \frac{\sum_i A_i \rho_i h_i}{\sum_i A_i \rho_i} = \frac{\sum_i A_i \rho_i h_i}{\overline{A}\,\overline{\rho}}$$

This scheme of averaging is a stable procedure because the divisor in the above equation is always nonzero, at least if all children densities are larger than zero.

6.2.2 Adaptive Algorithm

The adaptive algorithm calculates the gravity effect caused by a topographic grid on a set of gravity stations. If surface density data are available, they can be included as well. The gravity value returned by the algorithm is only an approximation of the "true" gravity value, which is defined as the gravity effect of layer 0 (i.e., in case of nonadaptive calculations at original resolution). The maximum acceptable deviation between true gravity value and the result of the algorithm is an input parameter called the *error tolerance*.

The second parameter of the adaptive algorithm is the "starting layer" j^*. It defines a maximum cell size and respectively a minimum resolution. The adaptive algorithm then refines the grid locally starting from this cell size. In principle, the refinement could start a layer n. Then, the entire grid is represented as a single block. However, when doing so, inaccurate results may be obtained (see tests in the next section). Setting an adequate maximum cell size stabilizes the algorithm.

Our algorithm is based on classic adaptive algorithms for numerical integration (e.g., Gander and Gautschi, 2000). Their central idea is to compute two estimates of an integral over a domain. One uses a coarse resolution, and another uses a finer resolution. Their difference provides a measure of the uncertainty/error of the estimates. If this estimate surpasses an error threshold, the domain is split, and the algorithm is applied recursively to all subdomains. This approach can be applied to the calculation of the mass correction, since it is essentially a form of integration as well.

The adaptive algorithm traverses the tree from top to bottom, beginning with the nodes of the starting layer j^*. For each node N in layer j^*:

1. Compute two gravity values: That of the node itself, and the total gravity of its four children.
2. Calculate the difference of those gravity values to get an estimate of the uncertainty of the gravity.
   a. If the uncertainty is higher than the layer error threshold (note: this is not the global error tolerance) try to split each children of N into their four children (the "grand-children" of N).
      i. If this is possible, recursively repeat steps 1 and 2 for all children of node N.
      ii. If node N has no grandchildren, the children of N are already from layer 0, and thus cannot be split. Save the gravity value and proceed to the next node of the starting layer j^*.
   b. If the uncertainty is below the local error threshold, save the gravity value and proceed to the next node of the starting layer j^*.

The layer error threshold is equal to the global error tolerance divided by the number of nodes each active layer. This procedure is repeated for each gravity station. All stations are processed completely independently. Stations can be located anywhere above the topography.

6.2.3 Forward Calculation of Gravity

The adaptive algorithm needs a way to compute the gravity value of a node in the quadtree. Since we assume a constant topographic height in each grid cell, each cell automatically corresponds to a tesseroid ("spherical prism"), because global DEMs are in geographic coordinates. There is no closed analytical expression for the gravity field of a tesseroid (Heck and Seitz, 2007), because the corresponding Newton-Integral is elliptical. However, the gravity effect of a tesseroid can be estimated using numerical methods (Grombein et al., 2013). Here, we use the adaptive Gauss−Legendre integration for a surface integral formulation of the Newton-Integral. Adaptive numeric integration allows calculating the gravity effect for each tesseroid to a specified accuracy.

Note that the adaptive approach itself is agnostic with respect to the elementary bodies. Replacing tesseroids by prisms, for example, would be straightforward. The only requirement is that the forward calculation for each elementary body can be determined accurately enough. Specifically, the accuracy of the forward calculation needs to be less than the smallest layer error tolerance. Otherwise, the errors of the forward gravity calculation would dominate, making error estimation (see step 2 of the algorithm) meaningless. Holzrichter (2013) has developed a similar adaptive algorithm that uses a polyhedral approximation of topography.

6.3 TEST OF ALGORITHM

The acceptance of the new approach depends on reliability and efficiency of the adaptive algorithm. Reliability means the true error does not exceed the error tolerance, while efficiency points to faster calculations—faster than calculations without adaptive change of resolution. Furthermore, the impact of the parameters (error tolerance and minimum resolution) on the results of the algorithm needs to be investigated. As a normal procedure, the new adaptive algorithm is tested by a "two-level" approach: the first bases on numerical experiments with synthetic topography and the second on a global topography model.

We will present two independent experiments. First, the quality of the error estimation was analyzed, using an in-depth Monte-Carlo analysis applied to synthetic topography. The implications from these synthetic tests were then verified using two real-world data sets.

6.3.1 Monte-Carlo-Analysis

We tested the error estimation using a Monte-Carlo approach on synthetic random topography. Accurate estimation of error is crucial for the success of the adaptive algorithm. Clearly, it would be best if the error estimate was perfectly accurate. Inaccurate estimation of error could cause two problems. If the error is underestimated, the algorithm will accept a resolution that is too crude, possibly returning an inaccurate gravity correction result. Overestimation, on the other hand, will slow the algorithm down. Since reliability trumps speed, mild overestimation is acceptable, but underestimation should be avoided.

To test how well the error is estimated, it is sufficient to study a small region, say no more than 32×32 cells. This small area is representative for the kind of decision the algorithm has to make during the calculation. By changing the nominal resolution of the test grid, scenarios representative for the higher layers of the quadtree can be tested. Thus, if the error estimation is acceptable for these small areas, it will be acceptable for larger grids as well. Creating synthetic topography for such small number of nodes is straightforward, and by adjusting the parameters controlling how topography is created, a wide range of plausible topographic environments can be studied.

We assume topography can be described by a Gaussian random field, having a constant expectation and an exponential isotropic covariance function:

$$C(d) = Se^{-3d/r}$$

where S is the "sill," r is the "range," and d is the distance between two points. The range r controls the smoothness of the synthetic topography: A higher range means the generated topography is more smooth. The height values of the synthetic topography are h_i. Under these assumptions, h_i have a multivariate normal distribution, from which samples can be drawn using standard techniques.

The parameters used for the Monte-Carlo study are as follows: two cell sizes (grid spacing) were used: 100 m and 10 km. The first resolution roughly corresponds to the resolution of Shuttle Radar Topography Mission (SRTM), which will be used in our real-world data test. The second resolution is typical for resolutions at the starting layer j^*. All grids were square, and the number of cells along each edge was either 4, 8, 16, or 32.

The sill was constant at 0.1 km^2 because we found that it acts as a scaling factor and has little impact on the algorithm's behavior. The range varied between 100 m and 10,000 km. The mean height of topography was 1 km. For each set of parameters (number of cells, size of each cell, range), 1000 random grids were generated. The total grid length is the product of cell size and number of cells per dimension. It is thus equal to the resolution of the grid cells at layer n, i.e., the root of the tree.

Gravity is calculated for a grid of stations placed 1 m above the center of each grid cell. (There is no specific reason for the 1 m station height option—all other station heights would also be feasible.) Note that the number of stations is equal to the number of grid cells. For each station, the gravity effect of layer n, $n-1$, and 0 was computed, giving g_n, g_{n-1}, and g_0. g_0 uses all available topographic information and is hence used as reference value.

g_n is an approximation of g_0, with an error $\epsilon = |g_n - g_0|$. The goal of the adaptive algorithm is to keep ϵ below the user-specified threshold. An estimate of ϵ can be obtained by taking the difference between g_n and g_{n-1}. This gives an estimated error $\tilde{\epsilon} = |g_n - g_{n-1}|$ for g_n. The adaptive algorithm can only function, if $\tilde{\epsilon}$ is not systematically underestimating ϵ.

We define the average success rate as the probability that the estimated error is larger than the true error because we want to avoid underestimation of error. The average success rate is calculated over all 1000 random grids and stations for each set of parameters. It will serve as a metric to evaluate the error estimation.

6.3.1.1 Results

6.3.1.1.1 Influence of the Range on Success Rate

Fig. 6.3 highlights the influence of the geostatistical range of the topographic grid on the average success rate. For low ranges, the average

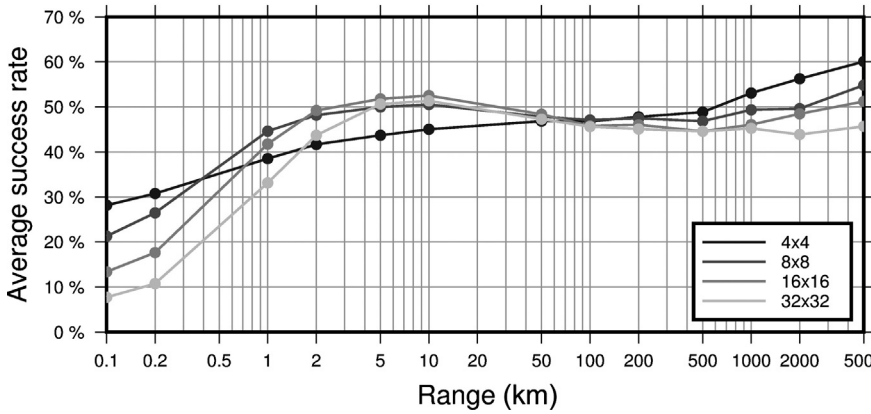

Figure 6.3 Result of the Monte-Carlo test for a cell size of 100 m. As the range of the topographic grid increases, the error estimate becomes more accurate. Once the range of the topography grid is above 10 km, the average success rate stays almost constant at around 50%. For small grids the success rate is higher because the algorithms need to extrapolate over less layers. However, for ranges above 10 km the differences between grid sizes become negligible. Therefore, the range exerts strong influence on the behavior of the adaptive algorithm.

success rate increases strongly with range, reaching a maximum of about 50% for ranges of 10 km. For ranges above 10 km, the success rate decreases again slightly. The success rates are similar for the different grid sizes, except 4×4, if the range is above 5 km.

When the cell size is increased by a factor of 100 to 10 km, the results scale consistently. That is, the maximum success is attained at a range of 1000 km, which is 100 times the threshold observed for the cell size of 100 m. However, the maximum success rate is reduced to 40%.

Results for all cell sizes, grid sizes, and ranges can be combined in an elegant way, by using the ratio of range to total grid length. This ratio will be called χ. Fig. 6.4 shows that χ exerts strong control over the average success rate. For $\chi < 3$, the average success rate increases with χ. This increase tapers off at $\chi = 3$, so that for $\chi > 3$ the success rate changes only slightly with χ. The success rate increases again when the ratio becomes larger than 1000, but such high values of χ are unlikely to appear in real world data.

As a first result, we conclude that the results of the Monte-Carlo method show that the ratio of the range to total grid length has critical impact on the quality of the error estimation. If this ratio is less than three, the adaptive algorithm suffers from systematic underestimation of error. Consequently, the minimum resolution of the adaptive algorithm should be chosen to be no more than one-third of the range of

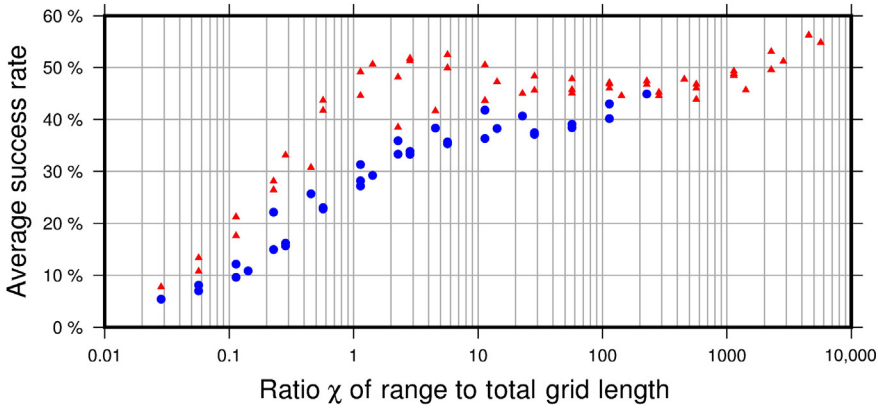

Figure 6.4 Results of the Monte Carlo tests as a function of χ. The blue dots (gray in print versions) belong to a cell size of 10 km, the red triangles to a cell size of 100 m. The behavior of the average success ratio is strongly controlled by χ. For χ larger than three, the average success is almost constant, except for extreme values of χ(>1000).

the topography. Whether or not a success rate of 50% (40%) is enough for practical applications will be tested in the next section.

6.3.2 Real World Data

After the numerical tests by aid of synthetic topography now we chose two real world datasets to test the adaptive algorithm: data which cover

- the Tibetan plateau and
- the globe

6.3.2.1 Tibetan Plateau

The first data set is a rectangular area in the Tibetan plateau (from 30°N to 33.5°N and 85°E to 88.5°E) as test bed for our algorithm (see Fig. 6.5). The area is challenging because the topographic characteristic of landscape varies substantially, showing both vast plains and ragged mountains. Furthermore, there are no oceans in this area, so we can use reprocessed SRTM data with a resolution of 90 m (Jarvis et al., 2008). The grid contains about 16 million data points. Geostatistical analysis of the area indicates constant mean height and an exponential, isotropic covariance function. The sill is around

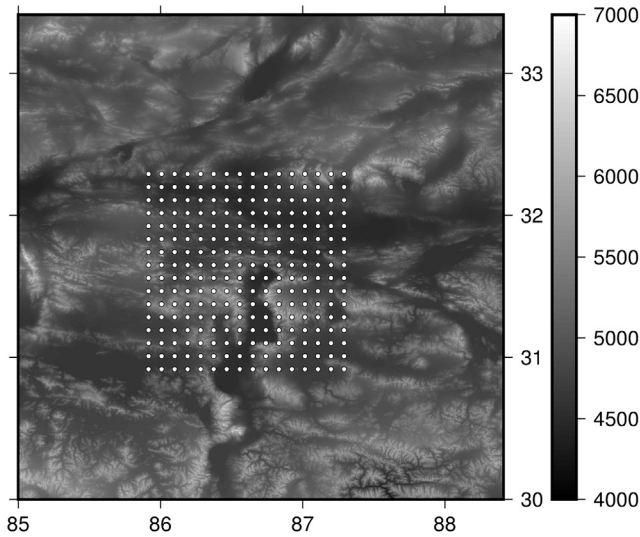

Figure 6.5 Topographical map of the test case in the Tibetan plateau. The color scale gives topographical height in meters. Each blue dot gives the location of a gravity station used in the test. Note that the stations are well removed from the edge of the topographical grid, so edge effects can be ignored (white in print versions).

0.1 km^2, and the range is up to 65 km, which is within the range of values used for the synthetic test. Therefore, the results from the synthetic approach can be applied.

We calculated the gravity effect for a grid of 16×16 stations in the center of the study area. The horizontal distance between stations is about 5 km, so the stations cover an area of roughly 90×90 km. The area covered by station is small compared to the size of the overall topography grid, so edge effects are negligible. The height of the stations is 1 m above topographical height extracted from the SRTM grid (refer also to comment at page 100).

Two experiments were carried out with this data set.

- First, the overall impact of the topography grid's resolution on the accuracy of the obtained gravity value was studied. This provides some guideline for choosing the error tolerance as a function of the grid resolution. However, this neglects other factors such as the measurement accuracy.
- Second, the adaptive algorithm was applied to the Tibetan data set, to how the parameters (error tolerance and maximum cell size) must be chosen to ensure reliability and efficiency.

6.3.2.2 Influence of Resolution

Each layer of the quadtree is a complete topographical grid at a certain resolution. Comparing the gravity effect of a layer with the true gravity value thus gives an estimate of the error incurred by using the resolution of that layer.

Fig. 6.6 shows the root-mean-square error over all 256 stations as a function of the cell size (resolution). For cell sizes below 20 km the error is roughly proportional to $l^{1.06}$, where l is the resolution. If the cell size is above 20 km, the average error changes very little and remains at about 22 mGal[1].

A least-square linear fit for cell sizes below 10 km gives the dashed black line in Fig. 6.6. This relation implies that at a resolution of 90 m, subscale variations cause an error in the order of 0.1 mGal. This represents an absolute lower bound on the errors, because all other causes of error are neglected. Thus, it makes little sense

[1] 1 mGal = 10^{-5} m/s^2.

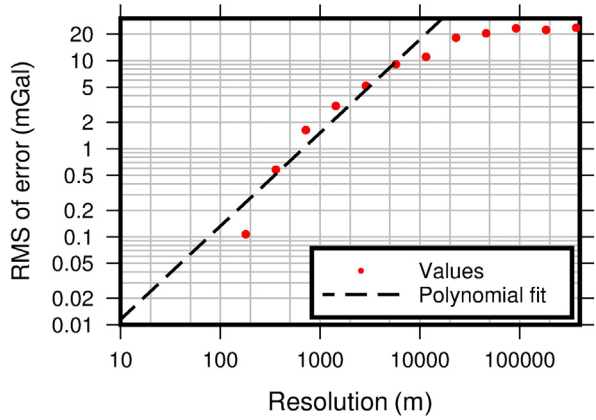

Figure 6.6 Average error relative to a resolution of 90 m. The dashed black line is obtained by fitting a polynomial function to the data points with resolution smaller than 20 km. Note that the RMS error for resolutions of 10 km or more changes very little compared to smaller cell sizes. This qualitative change in behavior is consistent with the results from the synthetic study. Thus, resolution and range of a topographic grid should be strongly connected.

to choose an error tolerance that is much lower than 0.1 mGal for this grid.

Furthermore, Fig. 6.6 corroborates the findings of the synthetic Monte-Carlo study. The error behavior changes qualitatively at a resolution of roughly 20 km, which with a range of $\sim$65 km coincides with $\chi \approx 3$. The explanation is that if the resolution is above 20 km, the gravity effects of the consecutive layers are very similar. Accordingly, if the adaptive calculation begins at one of these layers, the error estimate will be too small systematically, resulting in a reduced success rate.

6.3.2.3 Adaptive Algorithm

We tested the adaptive algorithm using a set of different parameters. The error tolerance varied between 0.01 and 100 mGal. The starting layer j^* was between 7 and 11, corresponding to maximum cell sizes of 12 to 190 km (2^7 to 2^{11} times the original grid resolution of 90 m). We calculated the gravity using the adaptive approach for all 256 stations for all combinations of the two parameters.

We calculated the maximum error over all stations. Each line in Fig. 6.7 shows how the maximum error changes as a function of the error tolerance, for a given maximum cell size. Points outside the gray

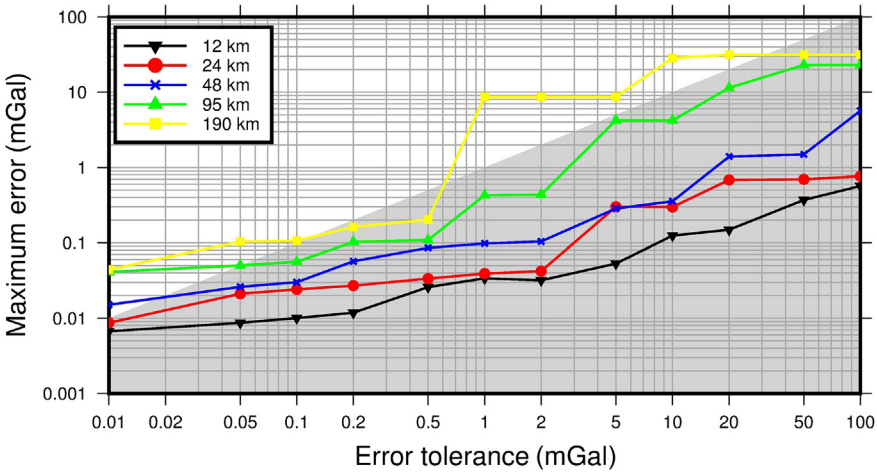

Figure 6.7 Maximum error of all stations as a function of the error tolerance. The shaded gray area is admissible because the maximum error is lower than the error tolerance. Outside of the gray area the accuracy requirement has not been met. Each line is for a different maximum cell size. Only a maximum cell size of 24 km or 12 km is admissible for all error tolerances.

area in Fig. 6.7 exceed the error tolerance. Thus, all lines should ideally lie within the gray area. However, only the curves for 24 and 12 km minimum resolution reliably achieve this. If the error tolerance can be larger than 0.1 mGal, minimum resolutions of 48 or 95 km are also acceptable.

The curve for 190 km shows somewhat erratic behavior: For a tolerance of 10 mGal, it surpasses the error threshold by a factor of three, while for a much stricter tolerance of 0.5 mGal it does not. This behavior can be explained by the fact that the maximum error is determined by a single station. Since we have only used 256 stations, it is mere coincidence that the achieved error drops. Still, the algorithm is not reliable with this maximum resolution.

This observation is consistent with our synthetic tests. As the range of the topographic grid is 65 km, we expect that the behavior of the algorithm changes at around 20 km (corresponding to $\chi = 3$). However, for medium error tolerances, the algorithm's performance is satisfactory even with much more lenient constraints on the maximum cell size (i.e., 95 km).

To judge the efficiency of the adaptive approach, we compare the average number of tesseroids used per station with the total number of

grid cells. The number of tesseroids counts tesseroids from all layers of the quad tree, not only those at the highest resolution/lowest layer. This gives an adequate metric for the adaptive approach because it accounts for the overhead of the adaptive algorithm. Also, the number of tesseroids used should be representative for the results obtained using any elementary body.

For a maximum cell size of 190 km, the number of tesseroids depends polynomially on the error tolerance: To decrease the error by a factor of 10, four times as many tesseroids are needed for calculations. As expected, enforcing smaller tesseroids by reducing the maximum cell size, increases the number of required tesseroids (Fig. 6.8).

However, for small error tolerances, the curves for different minimum resolutions converge. The maximum cell size also defines a minimum number of tesseroids. Thus, the number of tesseroids flattens out for large error tolerances (Fig. 6.8). Furthermore, the maximum number of tesseroids used per station was around 570,000. This is equal to 3.5% of the total number of cells in the grid. Even with the strictest accuracy requirements, the algorithm only needs to calculate 3.5% the number of tesseroids compared to the naïve approach.

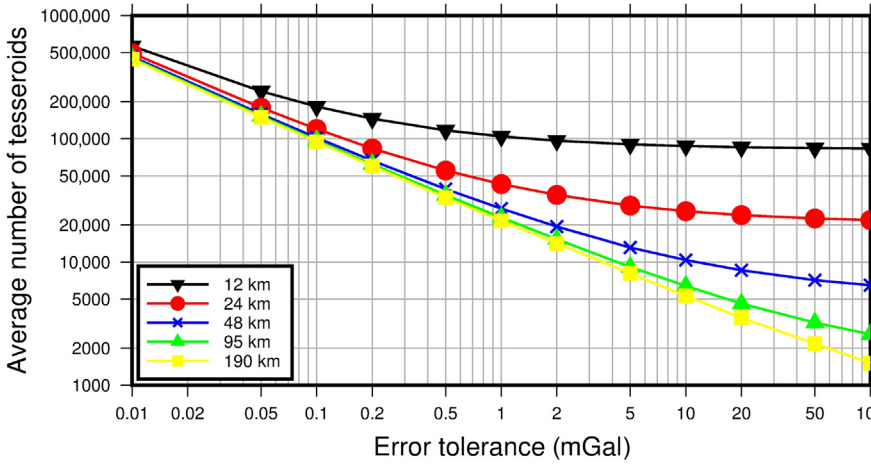

Figure 6.8 Average number of tesseroids used per station. Each line is for a different maximum resolution. Note that the number of tesseroids increases roughly polynomially with the error tolerance. However, the curves for small maximum cell sizes are flatter for larger error tolerances, because they have a higher minimum number of tesseroids. As the error tolerance becomes smaller the curves get closer together (although this effect is exaggerated by the logarithmic scaling). Hence, for strict error tolerances, the chosen maximum cell size has a small effect on the numeric efficiency.

6.3.2.4 Global Calculation

As second data set, we used ETOPO 1 (Amante and Eakins, 2009) a global topographic data set with a resolution of 1 arc min. Thus, there are about 233 million grid points in total. Geostatistical parameters range and sill are about 3000 km and 7 km^2, respectively, for this grid. Accordingly, minimum resolution was set to 1000 km. Gravity was calculated on a global grid of gravity station at a grid spacing of 1°. Station height is 1 m above topography onshore and 1 masl offshore. An error tolerance of 1 mGal was used for the adaptive calculation.

Fig. 6.9 shows the total mass correction obtained using the adaptive algorithm. A strong correlation with topography was expected, because the "Bouguer"-part of mass correction has a dominating influence. Our results agree with the global topographic effect calculated by (Balmino et al., 2012). In Fig. 6.10, the DRE has been isolated. This finding agrees well with the results of Mikuška et al. (2006) and underlines the need of taking distant topography into account. *However note that Mikuska et al. use a different sign convention compared to the results in* Fig. 6.10.

The gain in speed due to the adaptive algorithm is demonstrated by the number of tesseroids used during the calculation (see Fig. 6.11). At most 400,000 tesseroids are used, which is equivalent to 0.17% of the data points. These extreme values are limited to relatively small areas (i.e., the Tibetan plateau, the Eastern Pacific rim), and in most regions considerably less tesseroids are needed.

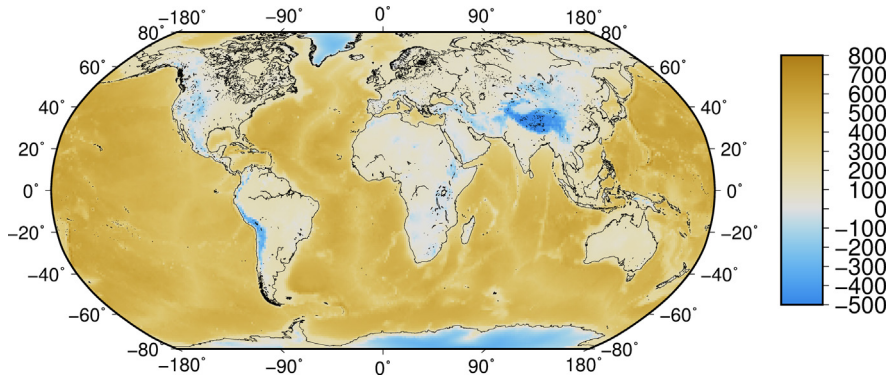

Figure 6.9 Mass correction in mGal 1 m above topography (sea level) calculated using ETOPO 1.

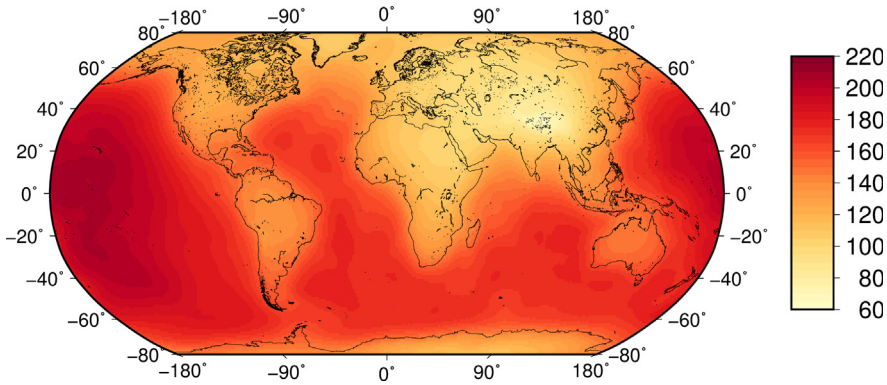

Figure 6.10 Distant Relief Effect in mGal 1 m above topography calculated using the ETOPO 1 model.

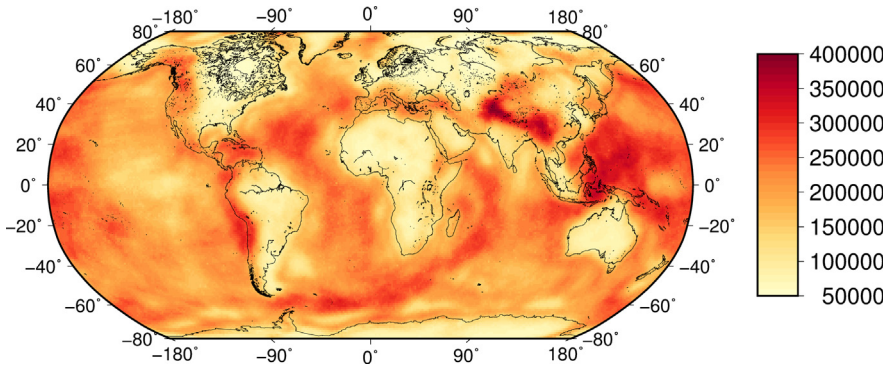

Figure 6.11 Number of tesseroids used, during the adaptive calculation with ETOPO 1. Note that ETOPO 1 model contains 233 million data points in total. Thus, the number of calculated tesseroids is less than 0.17% of the original number of grid cells. In most areas considerably less tesseroids are used. For instance, most of Africa requires less than 50,000 tesseroids, equivalent to 0.02% of original grid cells.

6.4 DISCUSSION

Based on our synthetic and real world test cases, we conclude that the adaptive algorithm is both reliable and efficient.

The "Tibetan" test using high-resolution (90 m) topographic data demonstrates that our adaptive approach is capable of reproducing the nonadaptive result with an accuracy 0.01 mGal, using only 3.5% of the grid cells. This precision is well below the uncertainties associated with modeling assumptions and measurement accuracy at continental scale. If the error tolerance is more lenient, the adaptive algorithm uses less grid cells, so that less than 1.3% of the grid cells are required for an accuracy of 0.1 mGal.

How much the number of tesseroids can be reduced depends on the following factors:

- The number of cells in the original grid, and thus the resolution and horizontal extent of the original grid. The amount of reduction is proportional to the number of cells.
- The minimum resolution sets a lower limit for the number of tesseroids.
- The error tolerance. Decreasing the error by a factor of 10 increases the number of tesseroids by 4.
- The geostatistical properties, most notably the range, affect the required resolution both directly and indirectly through the required minimum resolution.

The observed speed-ups were in the order of 30 (for the area of the Tibetan plateau) to 1000 (for global calculations).

Reliable behavior of the adaptive algorithm was ensured by requiring a maximum cell size. Using synthetic tests, we found that the relation between total grid length and geostatistical range exerts critical influence on the behavior of the algorithm. The algorithm estimates the error made by a coarse resolution effectively only if the ratio of range to total grid length is less than 3. Total grid length corresponds to the maximum cell size in the real world tests. Hence, the maximum cell size can be chosen according to the range of the study area. The validity of this approach was demonstrated in the "Tibetan" test case.

However, studies of synthetic cases are subject to a number of limitations. First, our geostatistical model was rather simple. We neglected anisotropy and spatial variability of mean height, range or sill; and used only a single (exponential) shape of the covariance function. Furthermore, we limited our test to Gaussian random fields, so we did not consider higher order moments, which are often necessary for an adequate description of real topography (Goff and Jordan, 1988). Second, the generated synthetic grids had a maximum dimension of 32×32, which is small compared with the extent of actual topography data. However, since the results for the Tibetan test case are consistent with the synthetic observations, we maintain that the geostatistical range can be used as a basis for choosing the required maximum cell size.

The efficiency of the algorithm is clearly demonstrated by the "Tibetan" test case and the results of the global calculation. As measure of efficiency, we use the number of tesseroids used compared to the original number of cells in the grid. We find that the adaptive algorithm causes some numerical overhead by constructing the quadtree and estimating the error, but it is still considerably faster than the naïve approach.

Adaptive algorithms provide an elegant way of combining high resolution and large lateral extent of topographic data. Thus, both distant and local gravity contributions of the topographic grid can be included. This makes them very attractive for surveys at regional scale. Furthermore, our adaptive approach is flexible. It can thus be directly applied to satellite or airborne gravity data as well as gravity gradient measurements.

ACKNOWLEDGMENTS

This study contributes to research which was done in the Priority Programme SPP 1257 "Mass transport and mass distribution". It has been financed by the Deutsche Forschungsgemeinschaft (DFG), grant (GO 380/27-1/2). We also thank A. Cogbill and one anonymous reviewer whose comments helped substantially to improve a first version of this manuscript.

REFERENCES

Amante, C. and B.W. Eakins (2009). ETOPO1 1 Arc-Minute Global Relief Model: Procedures, Data Sources and Analysis.

Balmino, G., Vales, N., Bonvalot, S., Briais, A., 2012. Spherical harmonic modelling to ultra-high degree of Bouguer and isostatic anomalies. J. Geod. 86 (7), 499–520. Available from: http://dx.doi.org/10.1007/s00190-011-0533-4.

Bouman, J., Ebbing, J., Meekes, S., Fattah, R.A., Fuchs, M., Gradmann, S., et al., 2015. GOCE gravity gradient data for lithospheric modeling. Int. J. Appl. Earth Observ. Geoinform. 35, 16–30.

Bullard, E.C., 1936. Gravity measurements in East Africa. Phil. Trans. R. Soc. A: Math. Phys. Eng. Sci. 235 (757), 445–531. Available from: http://dx.doi.org/10.1098/rsta.1936.0008.

Cogbill, A., 1990. Gravity terrain corrections using digital elevation models. Geophysics 55, 102–106.

Gander, W., Gautschi, W., 2000. Adaptive quadrature – revisited. Bit Numer. Math. 40 (1), 84–101. Available from: http://dx.doi.org/10.1023/A:1022318402393.

Goff, J.A., Jordan, T.H., 1988. Stochastic modeling of seafloor morphology: inversion of sea beam data for second-order statistics. J. Geophys. Res. 93 (B11), 13589. Available from: http://dx.doi.org/10.1029/JB093iB11p13589.

Grombein, T., Seitz, K., Heck, B., 2013. Optimized formulas for the gravitational field of a tesseroid. J. Geod. 87 (7), 645–660. Available from: http://dx.doi.org/10.1007/s00190-013-0636-1.

Hammer, S., 1939. Terrain corrections for gravimeter stations. Geophysics 4 (3), 184–194.

Hayford, J.F., Bowie, W., 1912. The Effect of Topography and Isostatic Compensation Upon the Intensity of Gravity. U.S. Coast and Geodetic Survey, Special Publication No. 10, 132 pp.

Heck, B., Seitz, K., 2007. A comparison of the tesseroid, prism and point-mass approaches for mass reductions in gravity field modelling. J. Geod. 81 (2), 121–136. Available from: http://dx.doi.org/10.1007/s00190-006-0094-0.

Holzrichter, N., 2013. Processing and Interpretation of Satellite and Ground Based Gravity Data at Different Lithospheric Scales, PhD Thesis. Kiel University, Kiel.

Jarvis, A., H.I. Reuter, A. Nelson, and E. Guevara (2008). Hole-Filled SRTM for The Globe Version 4, available from the CGIAR-CSI SRTM 90m Database (http://srtm.csi.cgiar.org)., http://srtm.csi.cgiar.org.

LaFehr, T.R., 1991. Standardization in gravity reduction. Geophysics 56 (8), 1170–1178. Available from: http://dx.doi.org/10.1190/1.1443137.

Mikuška, J., Pašteka, R., Marušiak, I., 2006. Estimation of distant relief effect in gravimetry. Geophysics 71 (6), J59–J69. Available from: http://dx.doi.org/10.1190/1.2338333.

Nabighian, M.N., Ander, M.E., Grauch, V.J.S., Hansen, R.O., LaFehr, T.R., Li, Y., et al., 2005. Historical development of the gravity method in exploration. Geophysics 70 (6), 63ND–89ND. Available from: http://dx.doi.org/10.1190/1.2133785.

Nagy, D., Papp, G., Benedek, J., 2000. The gravitational potential and its derivatives for the prism. Journal of Geodesy 74, 552–560.

Samet, H., 1990. The Design and Analysis of Spatial Data Structures. Addison-Wesley Series in Computer Science, Addison-Wesley, Reading, MA, p. 493.

Szwillus, W., 2014. Ein adaptives Verfahren zur Berechnung der Massenkorrektur, Master Thesis. Kiel University, Kiel.